3D landslide run out modelling using the Particle Flow Code PFC^{3D}

R. Poisel & A. Preh
Institute for Engineering Geology, Vienna University of Technology, Vienna, Austria

ABSTRACT: Rockfalls are modelled as the movements of single rock blocks over a surface or as the movement of a viscous mass over a surface (e.g. DAN). In reality a mass of discrete, interacting rock blocks is moving downslope. Thus the program PFC (Particle Flow Code) based on the Distinct Element Method was modified in order to model rock mass falls realistically in 3 dimensions based on physical relations. PFC models the movement and interaction of circular (2D) or spherical (3D) particles and wall elements using the laws of motion and of force - displacement. In the course of the calculation the contacts between particles and particles or particles and walls are detected automatically. The particles may be bonded together at their contact points, and the bondage can break due to an impact. For realistic modelling of the run out a viscous damping routine in case of a particle – wall contact was introduced. Numerical drop tests and back analyses of several rock mass falls provided appropriate damping factors. Thus, the movement types bouncing, sliding, rolling and free falling of single rock blocks and the interaction between the blocks occurring in a rock mass fall can be modelled realistically by using the adapted code of PFC. The application of this method is demonstrated by the example of Aknes (Norway).

1 INTRODUCTION

Landslide run outs are modelled as the movements of single rock blocks over a surface or as the movement of a viscous mass over a surface (e.g. DAN). In reality a mass of discrete, interacting rock blocks is moving downslope. Thus the program PFC (Particle Flow Code) based on the Distinct Element Method was modified in order to model landslide run outs realistically in 3 dimensions based on physical relations.

PFC models the movement and interaction of circular (2D) or spherical (3D) particles and wall elements using the laws of motion and of force - displacement. In the course of the calculation the contacts between particles and particles or particles and walls are detected automatically. The particles may be bonded together at their contact points, thus modelling a solid, and the bondage can break due to an impact. Thus, PFC can simulate not only failure mechanisms of rock slopes, but also the run out of a detached and fractured rock mass (Poisel & Roth 2004).

Rock mass falls can be modelled as an "All Ball model" and as a "Ball Wall model". An "All Ball model" simulates the slope as an assembly of balls bonded together. The simulation shows the failure mechanism of the slope due to gravity (Poisel & Preh 2004). After detachment of the moving mass, the run out is modelled automatically.

In the "Ball Wall model" the underlying bedrock is simulated by linear (2D) and planar (3D) wall elements (Roth 2003). Therefore, an estimate or a model of the failure mechanism of the slope (Preh 2004) and of the detachment mechanism is needed as an input parameter. However, in the "Ball Wall model" the detached mass can be modelled, using more and smaller balls with the same computational effort in order to approach reality better.

2 RUNOUT RELEVANT PARAMETERS

According to observations in nature, several kinds of movements of the rock fall process (Broilli 1974) have to be distinguished during the computation (Bozzolo 1987):

- free falling,
- bouncing,
- rolling and
- sliding.

In order to achieve an appropriate simulation of these different kinds of movements by PFC, some modifications have been necessary using the implemented programming language Fish.

2.1 *Free falling*

In order to model the free falling of blocks, neither the acceleration nor the velocity (ignoring the air resistance) is to be reduced during fall as a consequence of mechanical damping.

PFC applies a local, non- viscous damping proportional to acceleration to the movement of every single particle as a default. The local damping used in PFC is similar to that described by Cundall (1987). A damping-force term is added to the equations of motion, so that the damped equations of motion can be written

$$F_{(i)} + F^{d}_{(i)} = M_{(i)}A_{(i)}; \quad i = 1\ldots6 \tag{1}$$

$$M_{(i)}A_{(i)} = \begin{cases} m\ddot{x}_{(i)} & \text{for } i = 1\ldots3; \\ I\dot{\omega}_{(i-3)} & \text{for } i = 4\ldots6 \end{cases} \tag{2}$$

where $F_{(i)}$, $M_{(i)}$, and $A_{(i)}$ are the generalized force, mass, and acceleration components, I is the principal moment of inertia, $\dot{\omega}$ is the angular acceleration and $\ddot{x}$ is the translational acceleration; $F_{(i)}$ includes the contribution from the gravity force; and $F^{d}_{(i)}$ is the damping force

$$F^{d}_{(i)} = -\alpha\left|F_{(i)}\right|\text{sign}(v_{(i)}) \quad i = 1\ldots6 \tag{3}$$

expressed in terms of the generalized velocity

$$v_{(i)} = \begin{cases} \dot{x}_{(i)} & \text{for } i = 1\ldots3; \\ \omega_{(i-3)} & \text{for } i = 4\ldots6. \end{cases} \tag{4}$$

The damping force is controlled by the damping constant α, whose default value is 0.7 and which can be separately specified for each particle.

This damping model is the best suited for a quick calculation of equilibrium. There arises, however, the disadvantage of the movements of the particles being damped as well. Therefore, the local damping has been deactivated for all kinds of particle movements.

2.2 *Bouncing*

Elastic and plastic deformations occur in the contact zone during the impact of a block. Both the kinetic energy of the bouncing block and the rebound height are reduced by the deformation work. The reduction of the velocity caused by the impact is modelled with the help of a viscous damping model integrated in PFC.

The viscous damping model used in PFC introduces normal and shear dashpots at each contact (Fig. 1). A damping force, D_i (i = n: normal, s: shear), is added to the contact force, of which the normal and shear components are given by

$$D_i = C_i \cdot |V_i| \tag{5}$$

where C_i (i = n: normal, s: shear) is the damping constant, V_i (i = n: normal, s: shear) is the relative velocity at contact, and the damping force acts to oppose motion. The damping constant is not specified directly; instead, the critical damping ratio β_i (i = n: normal, s: shear) is specified, and the damping constant satisfies

$$C_i = \beta_i \cdot C_i^{crit} \tag{6}$$

where C^{crit}_i is the critical damping constant, which is given by

$$C_i^{crit} = 2m\omega_i = 2\sqrt{mk_i} \tag{7}$$

where ω_i (i = n: normal, s: shear) is the natural frequency of the undamped system, k_i (i = n: normal, s: shear) is the contact tangent stiffness, and m is the effective system mass.

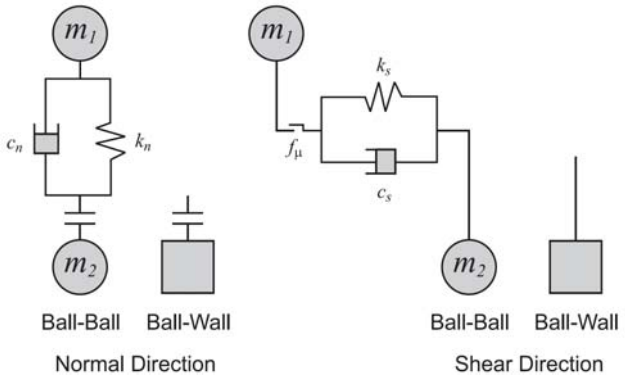

Figure 1. Viscous damping activated at a contact with the linear contact model (Itasca 1999)

In rock fall programs, the rebound height of blocks touching the bedrock is calculated using restitution coefficients. The restitution coefficient R_i (i = n: normal, s: shear) is defined as the ratio of the contact velocity before and after the impact and can be defined as

$$R_i = \frac{v_i^f}{v_i^i} \tag{8}$$

where v_i^f (i = n: normal, s: shear) is the velocity of the block after impact and v_i^i (i = n: normal, s: shear) is the velocity of the object before impact. The relation between the restitution coefficient R_i and the critical damping ratio β_i can be estimated by simulating drop tests (Preh & Poisel 2007).

Spin has an impact on both the direction and the velocity of the rebounding block. Therefore, it is essential to consider the spinning when modelling the run outs of rock falls. PFC determines the motion of each single particle by the resultant force and moment vectors acting upon it, and describes it in terms of the translational motion of a point in the particle and the rotational motion of the particle (Equations 1 and 2). Figure 2 depicts the flight trajectories of three particles bouncing at different spins.

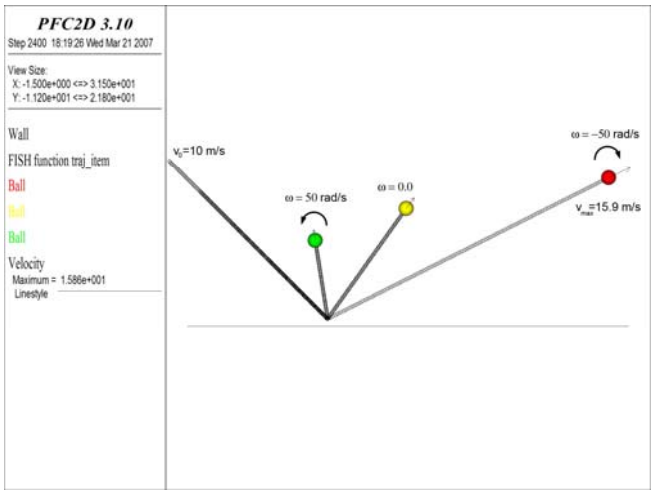

Figure 2. Rebound angle influenced by the particle spin (black line – rebound course; green, yellow and red balls – particle position after rebound)

Furthermore, with PFC the interaction of friction and spin is considered, since the influence of the spin increases with the increase of frictional resistance.

By modelling rock mass falls, it was shown to be necessary to distinguish between ball-ball contacts and ball- wall contacts. This was done by using the programming language Fish.

2.3 *Rolling*

The most important run out relevant effect is rolling resistance, because it is known that pure rolling of blocks in the model leads to more extensive run outs than observed in nature.

The rolling resistance is caused by the deformation of the rolling body and/or the deformation of the ground (Fig. 3) and depends strongly on the ground and the block material.

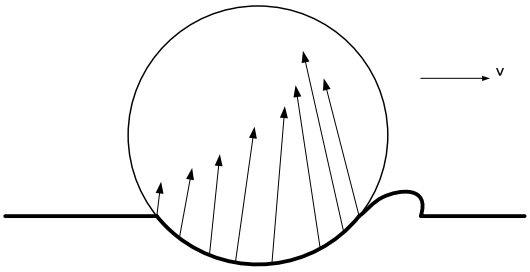

Figure 3. Deformation of the surface and distribution of contact stresses

Due to these deformations, the distribution of contact stresses between the ground and the block is asymmetric (Fig. 4). Replacing the contact stresses by equivalent static contact forces results in a normal force N, which is shifted forward by the distance of c_{rr} , and a friction force F_{rr} , opposing the direction of the movement.

The deceleration of the angular velocity caused by the rolling resistance is calculated using conservation of translational momentum (Equation 9) and angular momentum (Equation 10).

$$m \cdot \ddot{x}_s = -F_{rr} \tag{9}$$

$$-I \cdot \dot{\omega}_{rr} = M_{rr} \ , \ I_{sphere} = \frac{2}{5} \cdot m \cdot r^2 \tag{10}$$

where M_{rr} is the resulting moment caused by the rolling resistance, I is the principal moment of inertia and ω_{rr} is the angular deceleration.

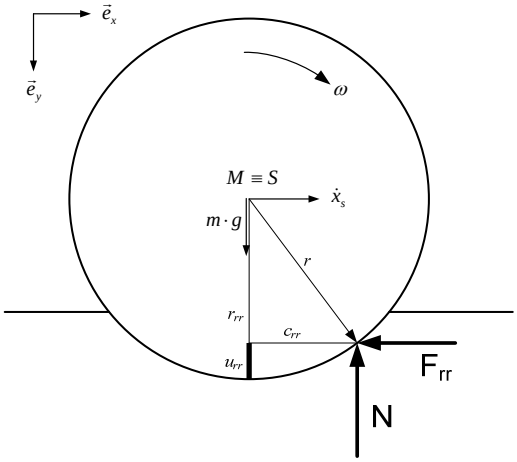

Figure 4. Calculation of the rolling resistance

The kinematic link is established by the condition of pure rolling (Equation 11).

$$\ddot{x}_s = \dot{\omega} \cdot r \tag{11}$$

The angular acceleration is defined by a finite difference relation in order to express the increment of the angular velocity per time increment (Equation 12). Thus, the friction force $F_{rr\ i}$is defined by the conservation of momentum

$$F_{rr} = -m \cdot \frac{\Delta\omega_{rr}}{\Delta t} \cdot r \tag{12}$$

Equation 10 and equation 12 yield

$$-\frac{2}{5} \cdot m \cdot r^2 \cdot \frac{\Delta\omega_{rr}}{\Delta t} = F_{rr} \cdot r_{rr} - N \cdot c_{rr} \tag{13}$$

$$-\frac{2}{5} \cdot m \cdot r^2 \cdot \frac{\Delta\omega_{rr}}{\Delta t} = -m \cdot \frac{\Delta\omega_{rr}}{\Delta t} \cdot r \cdot r_{rr} - m \cdot g \cdot c_{rr} \ .$$

Therefore, the angular deceleration is

$$\Delta\omega_{rr} = \frac{-g \cdot c_{rr}}{r \cdot (r_{rr} - \frac{2}{5} \cdot r)} \cdot \Delta t \tag{14}$$

$$r_{rr} = \sqrt{r^2 - c_{rr}^2} \ .$$

The rolling resistance is implemented by adding the calculated increment of the angular velocity to the angular velocity calculated automatically by PFC at every time step (Equation 14).

$$\omega_i^{(t)} = \omega_i^{(t)} + \Delta\omega_{rr,i} \tag{15}$$

According to these considerations, the rolling resistance is an eccentricity c_{rr} or sag function u_{rr}. The deeper the block sags, the greater is the rolling resistance $\Delta\omega_{rr}$. In classical mechanics, the rolling resistance is a function of the ratio of the eccentricity c_{rr} to the radius r.

$$\mu_r = \frac{c_{rr}}{r}[-] \qquad (16)$$

This means that spherical blocks of different sizes have the same run out for the same rolling resistance coefficient.

In nature, however, it can be observed that large blocks generally have a longer run out than smaller ones. Therefore, according to the damping model described, the run out is calibrated by the sag u_{rr}.

Calculations carried out by PFC, using the model of rolling resistance described above and modelling a detached rock mass as an irregular assembly of particles of two different sizes (r_1 = 0.8 m, r_2 = 1.6 m) employing the same sag of u_{rr}= 25 cm for both particle sizes have shown that the larger particles have a longer run out than smaller ones and that within the deposit mass the smaller particles (r = 0.8 m) rest at the bottom and the larger particles (r = 1.6 m) at the top (Preh & Poisel 2007). This model behaviour corresponds closely to observations in nature.

2.4 *Sliding*

Sliding is calculated by the slip model implemented in PFC without any further adaptation.

3 THE AKNES ROCK SLOPE FAILURE

Large rock slope failures are common events in the inner fjord areas of western Norway and represent one of the most serious natural hazards in Norway. Rock avalanches and related tsunamis (Harbitz et al. 1993) have caused serious disasters and during the last 100 years more than 170 people have lost their lives in western Norway. The Tafjord disaster occurred in 1934 when 3 million m³ rock mass dropped into the fjord. The tsunami generated by the avalanche reached a maximum of 62 m above sea level, several inhabited villages along the fjord were destroyed and 41 people were killed (Blikra et al. 2005).

The unstable rock slope at Aknes (Fig. 5) is situated in a remote area in a steep mountain slope and is built up by gneisses with an overall dipping foliation parallel to the slope (Tveten et al. 1998). The slide planes are probably following weak zones along the foliation planes. Geophysical data from 2D resistivity, refraction and reflection seismics and penetrating radar indicate that the slide is covering an area of some 800.000 m² maximum and that the thickness of the unstable area is between 40 and 140 m (Blikra et al. 2005).

The Aknes/Tafjord project was initiated in 2004 with the aim of investigating, monitoring and providing early warning of the unstable areas at Aknes and Hegguraksla in Tafjord in More and Romsdal County. The monitoring system includes extensometers, lasers, GPS, a total station, ground based radar and borehole instrumentation (Harbitz 2007). The displacement velocities are in the order of 3 – 10 cm/year at present. The geometry and structure of the failure is complex and the instable area seems to be composed of several individual blocks.

Figure 5. The Aknes rock slope.
Unstable area marked by dashed line.
Photo: Th. Sausgruber

Based on the relatively frequent slide events documented in the fjord areas, it has been estimated that a flank collapse at Aknes in the order of 1 – 8 million m³ may have a probability of less than 1 event /1.000 years (Blikra et al. 2005).

3.1 *Numerical investigations of the Aknes run out using PFC*

The unstable area at Aknes is divided into several scenarios, the smallest of which has a volume of some 5 million m³. The run out of this scenario was simulated using the PFC routine described above in order to assess the possible damage. The digital terrain models (DTMs) of the present terrain surface and of the detachment surface have been provided by NGI. These DTMs were used to generate the wall elements simulating the detachment and the terrain surface (Fig. 6) and the detached rock volume was modelled by 2583 particles (balls) with r_{min} = 5 m and r_{max} = 7.5 m (Fig. 7).

First it was assumed that the moving mass is fractured completely due to the sliding displacements before the run out starts. Thus the run out process of completely unbonded particles was started by deleting the wall elements above the detached rock volume.

Figure 8 shows the position of the unbonded particles at the moment the first particle hits the water surface, figure 9 the accumulated mass of particles hitting the water surface over time.

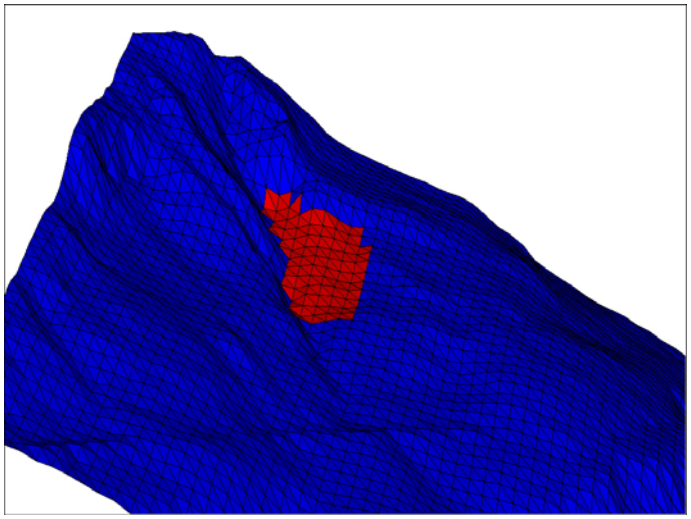

Figure 6. Detachment and terrain surface of the smallest scenario modelled by wall elements.

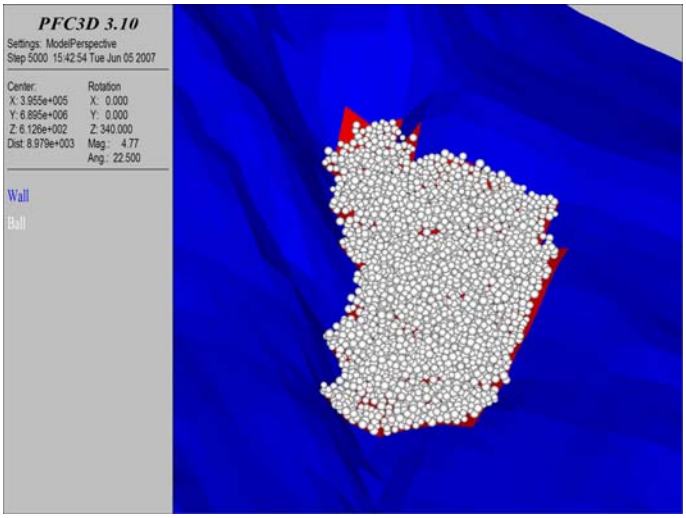

Figure 7. Detached rock volume modelled by 2583 particles.

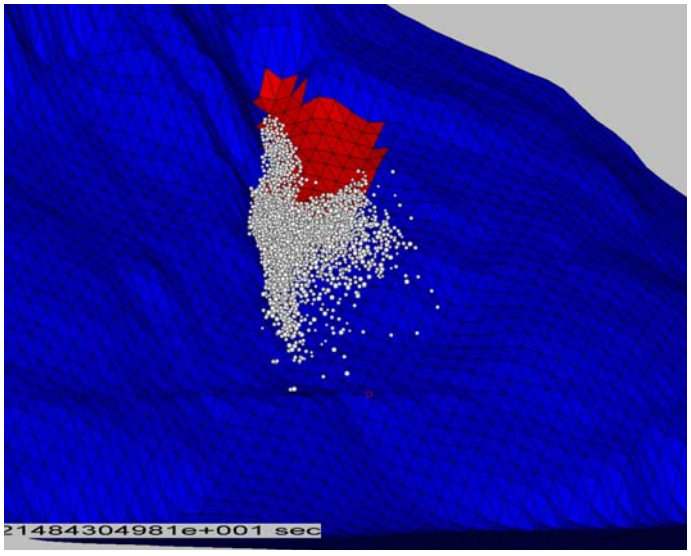

Figure 8. Unbonded material, distribution of particles at the moment the first particle hits the water surface

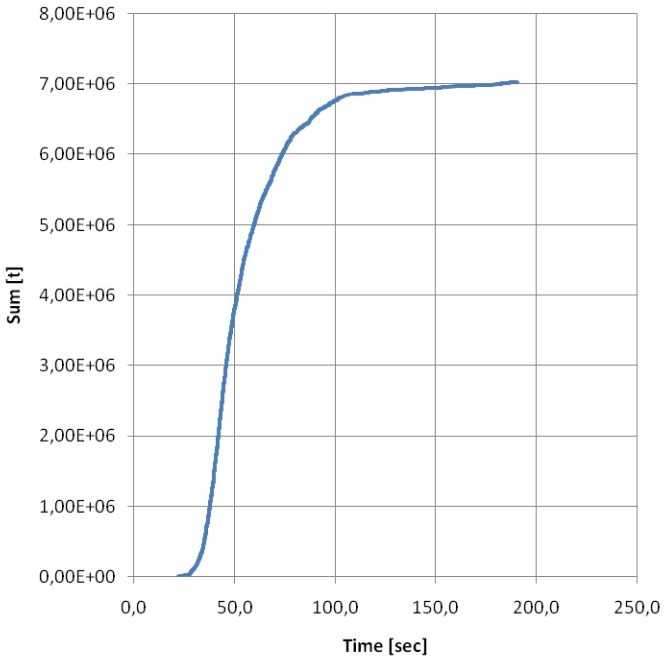

Figure 9. Unbonded material, accumulated mass of balls hitting the water surface over time

In a second approach it was assumed that the moving mass is composed of several blocks built up by an assemblage of particles. Thus bonds with a shear strength of 1 GN and with a tension strength of 1 GN were introduced at the particle contact points. These bonds partly broke during the following run out.

Figure 10 shows the position of the initially completely bonded particles at the moment the first particle hits the water surface, figure 11 the accumulated mass of particles hitting the water surface over time.

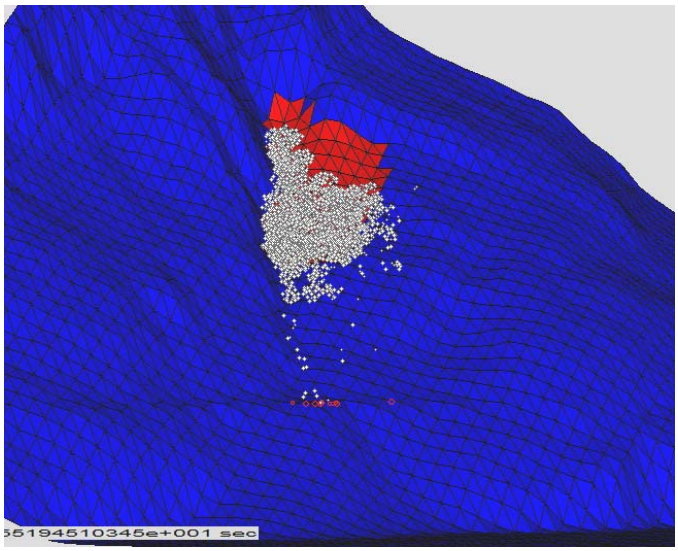

Figure 10. Bonded material, distribution of particles at the moment the first particle hits the water surface

Comparison of Figures 8 – 11 reveals completely different distributions in space as well as in time. The impacts of the unbonded material are restricted

more or less to the channel on the orographic right side of the moving mass while the initially completely bonded material runs down distributed over the whole width of the sliding mass. The run out of the unbonded material lasts only some 100 seconds, the run out of the initially bonded material some 400 seconds.

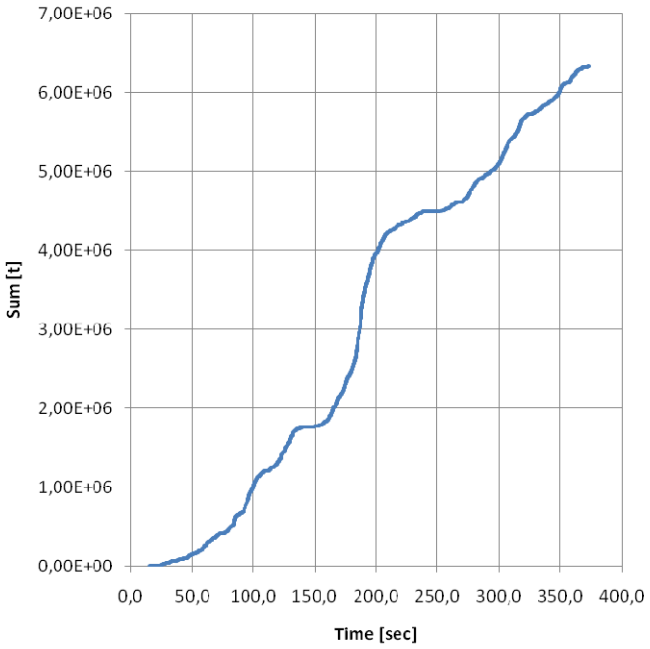

Figure 11. Bonded material, accumulated mass of balls hitting the water surface over time

The numerical simulation of the tsunami caused by the unbonded rock mass run out described above by Pastor (2007) showed that

- the wave height at the impact area is 20 m maximum,
- the wave height in the middle of the fjord (that is in open water) is 10 m maximum and
- the wave run up height along the opposite shore is 30 m maximum.

4 CONCLUSION

With the help of the adapted PFC code it is possible to create a mechanically correct model of rock mass falls in 3D. The adapted code was used to model the run out of the Aknes rock slide in the Geiranger Fjord (Norway) by unbonded and by bonded particles. The simulations showed different particle distributions in space and time which are expected to cause different tsunamis. Thus investigations of the sliding rock mass disintegration as a function of sliding displacements are essential.

REFERENCES

Blikra, L. H., Longva, O., Harbitz, C.B., Lovholt, F. 2005. Quantification of rock avalanche and tsunami hazard in Storfjorden, western Norway. In K. Senneset, K. Flaate, J.O. Larsen (eds.), *Landslides and avalanches. Proc. of the 11th Int. Conf. and Field Trip on Landslides (ICFL), Norway, September 1-10, 2005*: 57-63. London: Taylor and Francis.

Bozzolo, D. 1987. Ein mathematisches Modell zur Beschreibung der Dynamik von Steinschlag. *Dissertation Nr. 8490 an der ETH Zürich.*

Broilli, L. 1974. Ein Felssturz im Großversuch. *Rock Mechanics,* Suppl. 3: 69-78.

Cundall, P.A. 1987. Distinct Element Models of Rock and Soil Structure. In E. T. Brown (ed.), *Analytical and Computational Methods in Engineering Rock Mechanics*: Ch. 4, 129-163. London: Allen & Unwin.

Harbitz, C.B., Pedersen, G., Gjevik, B. 1993. Numerical simulations of large water waves due to landslides. *J. of Hydraulic Engineering* 119 (12): 1325-1342.

Harbitz, C.B. 2007. Personal communication.

Hoek, E. 1987. Rockfall – A program in basic for the analysis of rockfalls from slopes. Dept. Civil Eng., University of Toronto, Toronto.

Itasca 1999. PFC^{2D} (Particle Flow Code in 2 Dimensions) User's Guide. Itasca Consulting Group, Inc., Minneapolis.

Pastor, M. 2007. Numerical simulation of the tsunamis caused by the Aknes rock slide due to run outs modelled by PFC. Unpublished report.

Poisel, R. & Preh, A. 2004. Rock slope initial failure mechanisms and their mechanical models. *Felsbau* 22: 40-45.

Poisel, R &, Roth, W. 2004. Run Out Models of Rock Slope Failures. *Felsbau* 22: 46-50.

Preh, A. 2004. Modellierung des Verhaltens von Massenbewegungen bei großen Verschiebungen mit Hilfe des Particle Flow Codes. *PhD Dissertation,* Inst. for Eng. Geology, Vienna University of Technology.

Preh, A. & Poisel, R. 2007. 3D modelling of rock mass falls using the Particle Flow Code PFC^{3D} . *Proceedings of the 11th Congress of the International Society for Rock Mechanics, Lisbon, July 9-13, 2007. Specialized Session S01 – Rockfall – Mechanism and Hazard Assessment.*

Roth, W. 2003. Dreidimensionale numerische Simulation von Felsmassenstürzen mittels der Methode der Distinkten Elemente (PFC). *PhD Dissertation*, Inst. for Eng. Geology, Vienna University of Technology.

Spang, R.M. & Rautenstrauch, R.W. 1988. Empirical and mathematical approaches to rockfall protection and their practical applications. *Proceedings of the 5th International Symposium on Landslides, Lausanne, 1988:* Vol. II, 1237-1243.

Tveten, E., Lutro, O., Thorsnes, T.1998. Bedrock map Alesund. 1:250,000. Geological Survey of Norway.